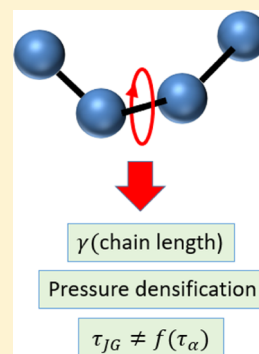


# Chain Flexibility and the Segmental Dynamics of Polymers

Daniel Fragiadakis\*<sup>1</sup> and C. Michael Roland<sup>1</sup>

Chemistry Division, Naval Research Laboratory, Washington, District of Columbia 20375-5342, United States

**ABSTRACT:** Using molecular dynamics simulations, we examine the dynamics of a family of model polymers with varying chain length and torsional potential barriers. We focus on features of the dynamics of polymers that are seen experimentally but absent in simulations of freely rotating and freely jointed chains. The reduced effect of volume on the segmental dynamics with increasing chain length, a capacity for pressure densification, and the deviation from constant Johari–Goldstein relaxation time at a constant segmental relaxation time all have a common origin, torsional rigidity, and these effects become increasingly apparent for more rigid chains.



## INTRODUCTION

With respect to their segmental dynamics, polymers in the supercooled regime are virtually indistinguishable from their small-molecule counterparts. At frequencies beyond terminal flow and the Rouse modes, the segmental relaxation of polymers has spectral shapes, temperature and pressure dependences, physical aging behavior, and dynamic heterogeneity that are qualitatively equivalent to those properties of molecular liquids. The class of “simple” liquids, per the isomorph description of Dyre and co-workers,<sup>1</sup> encompassing nonassociated molecular liquids also seems to include most polymers.<sup>2</sup> Both polymers and molecular liquids conform to density scaling; that is, the relaxation time  $\tau_\alpha$  and transport properties can be expressed as a function of the ratio of temperature and density, the latter raised to a material constant  $\gamma$ :  $\tau_\alpha = f(\rho^\gamma/T)$ . The exponent  $\gamma$  is related to the steepness of the intermolecular potential and quantifies the relative influence of temperature and volume on dynamics.<sup>3–7</sup>

While the flexibility of polymers chains can have a profound effect on certain physical properties, motion encompassing many repeat units is largely independent of the chemical structure.<sup>8</sup> Although introducing bending and torsional potentials slows down local relaxation, increasing the glass transition temperature, and affects the degree of chain entanglement, the qualitative nature of the dynamics does not change.<sup>9,10</sup> Thus, in computer simulations investigating polymer dynamics, freely jointed or freely rotating chains of Lennard-Jones particles are widely used.<sup>11</sup> Like their small-molecule counterparts, these simple models are attractive since they are much more computationally efficient than atomistic models but also lack chemical specificity and therefore might provide a more general understanding of glass-forming systems.<sup>12</sup> However, simulated freely jointed and freely rotating chains lack three dynamic properties, at first glance unrelated, that are observed experimentally for real polymers:

- (1) The density scaling exponent  $\gamma$  decreases with the chain length;<sup>13–15</sup> i.e., the dynamics in higher molecular-weight polymers is less sensitive to volume.
- (2) Polymers pressure-densify: vitrification under pressure yields higher densities than those of conventional glasses formed at ambient pressure.<sup>16,17</sup>
- (3) The Johari–Goldstein (JG) secondary relaxation time,  $\tau_{JG}$ , typically constant at fixed  $\tau_\alpha$  for molecular liquids becomes smaller for polymers at constant  $\tau_\alpha$ .<sup>18,19</sup>

## COMPUTATIONAL DETAILS

We simulate a family of chains based on Lennard-Jones particles with the size parameter and potential well depth set to unity. Bond lengths and angles are kept constant to within a few percent using harmonic potentials: neighboring segments are linked by harmonic bonds with length 0.5 and force constant  $10^5$ ; for the bond angle potential, the equilibrium angle was  $120^\circ$  with a spring constant 1000. We determined that the results are qualitatively independent of the force constants used (values of  $10^2$ – $10^4$  were tested). In addition, for chain lengths  $N > 3$ , a sinusoidal torsional potential was used to introduce chain rigidity

$$U(\theta) = 0.5A(1 + \cos 3\theta) \quad (1)$$

where  $\theta$  is the dihedral angle and  $A$  the barrier height. For a freely rotating chain,  $A = 0$ . For a freely jointed chain, the angle potential is also absent. In this work, we vary  $A$  to investigate specifically chain flexibility, i.e., the effect that the torsional potential governing rotation about backbone bonds has on the supercooled dynamics, in particular, the three properties enumerated above.

Received: April 30, 2019

Revised: June 12, 2019

Published: June 12, 2019

Approximately, 8000 Lennard-Jones particles (the closest multiple of the chain length) were simulated for each system. Molecular dynamics simulations were carried out in the NPT ensemble, using RUMD software<sup>20</sup> with a Nosé–Hoover thermostat;<sup>21</sup> the software was also modified to incorporate a Berendsen barostat.<sup>22</sup> For the heating and cooling ramps employed to study pressure-densified systems, we set the barostat time constant to be short enough (determined by trial and error) that the target pressure was accurately maintained throughout.

We consider a system fully equilibrated when the chain end-to-end correlation function has decayed to near zero. For long chains and low temperatures, it is sometimes impractical to wait for full equilibration. In those cases, we first fully equilibrate a system at the target density and higher temperature and then decrease the temperature and equilibrate for a time at least 100 times longer than the segmental relaxation time. We determined that this was sufficient for the static (density or pressure, potential energy) and dynamic properties ( $\alpha$  and end-to-end relaxation times) to no longer exhibit any time dependence.

For selected state points of the  $N = 100$  and 400 systems, we ran simulations of a larger system (32 000 particles) to assess size effects and found no significant difference in the segmental dynamics.

## RESULTS AND DISCUSSION

Along the glass transition or any other line of constant relaxation, the density scaling property can be expressed as<sup>23</sup>

$$T\rho^{-\gamma} = \text{constant} \quad (2)$$

More accurately, the reduced relaxation time  $\tilde{\tau}_\alpha^{24,25}$  should be used, defined as

$$\tilde{\tau}_\alpha = v^{-1/3}(kT/m)^{1/2}\tau_\alpha \quad (3)$$

where  $m$  and  $v$  are the molecular mass and volume, respectively.

Thus, double logarithmic plots of  $T$  versus inverse  $\rho$  at a constant reduced relaxation time should be straight lines having a slope equal to  $\gamma$ . Such plots are shown in Figure 1 for chains of various lengths  $N$  and torsional barrier height  $A$ ; the sets of state points with constant relaxation time were found by

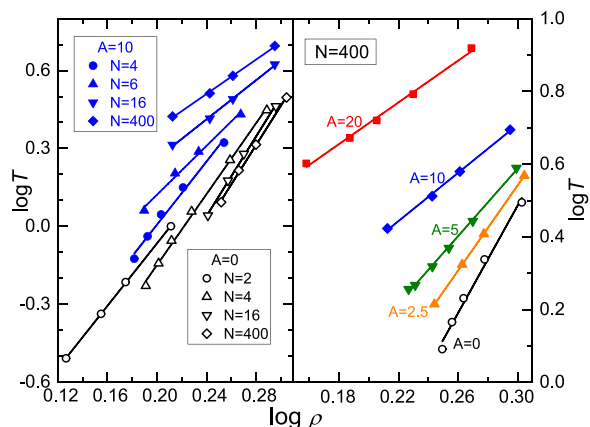


**Figure 1.** Double logarithmic plot of the temperature and density along an isochrone with  $\tilde{\tau}_\alpha \approx 10^3$  for the indicated simulated polymers. The slope of the fitted lines equals the density scaling exponent  $\gamma$ .

trial and error. The data for the most and least flexible chains with  $N = 400$  in Figure 1 have some curvatures; that is,  $\gamma$  is weakly density dependent.

In Figure 2 is plotted the mean  $\gamma$  as a function of the chain length for values of  $A$  from 0 to 20. For  $A = 0$  (freely rotating

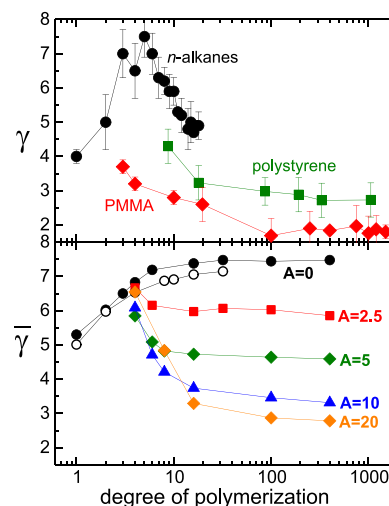


**Figure 2.** (Upper) Experimental density scaling exponent for polymers as a function of the number of repeat units. *n*-alkane data is from ref 24; poly(methyl methacrylate) PVT data is from ref 13 and reanalysis of data from refs 28–31; polystyrene is from analysis of PVT data.<sup>30,32,33</sup> (Lower) Average density scaling exponent vs number of repeat units for the simulated polymers having the indicated torsional potential barrier  $A$ . The empty symbols are for the freely jointed chain of ref 26.

chains),  $\gamma$  increases systematically with increasing chain length and saturates at  $N = 20$ . The values of  $\gamma$  are similar to those found by Veldhorst<sup>26</sup> for a freely jointed chain with rigid bonds longer by a factor of 2. The interpretation was that the rigid bonds can be seen as an infinitely steep repulsive potential that increases the effective steepness of the intermolecular potential. We recently found that the increase in  $\gamma$  from atomic to molecular and polymeric liquids based on the same interatomic potential can be quantitatively related to the molecular shape, which determines the scaling of the relevant intermolecular distance with density.<sup>27</sup>

An increasing exponent is opposite of the behavior seen experimentally in polymers, where  $\gamma$  decreases with the molecular weight up to an asymptotic limit,<sup>13–15</sup> leading to generally lower values of  $\gamma$  for polymers than for molecular liquids. Also included in Figure 2 are collected experimental results for polystyrene, poly(methyl methacrylate), and *n*-alkanes. These include new values from reanalysis of previously reported volumetric data, where  $\gamma$  is determined from the density  $\rho_g$  and temperature  $T_g$  at the glass transition, which are related by  $T_g\rho_g^{-\gamma} = \text{const}$  (eq. 2). We find that  $\gamma$  decreases with the molecular weight, the only exception being the very short *n*-alkanes, for which an increase in  $\gamma$  is seen from  $N = 1$  to 5. Introducing stiffness into the simulated polymers, the dependence on  $N$  decreases, in accord with the experimental behavior. This decrease is steeper for stiffer chains and levels off at a lower value of  $\gamma$  and at a higher chain length. A torsional potential only exists for  $N > 3$ , so a maximum in  $\gamma$  occurs at  $N = 3$  or 4, depending on chain rigidity, similar to the behavior of the *n*-alkanes.

Another property common to polymers is pressure densification (PD).<sup>16,17</sup> This refers to the formation of a glass by pressurizing the material prior to cooling below  $T_g$  and releasing the pressure; conventional glass (CG) is formed by simply cooling at ambient pressure. The PD glass has higher density and other properties that differ from CG. The freely jointed polymer cannot be pressure-densified; its density is equivalent to that of the glass formed at low pressure.<sup>34</sup> In Figure 3 are shown for simulated chains having varying

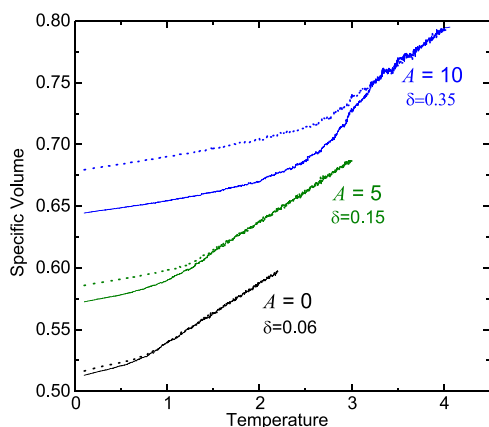


**Figure 3.** Volume at  $P_0 = 1$  during heating of the glass formed at  $P_1 = 1$  (dotted lines) and  $P_1 = 10$  (solid lines) for a freely rotating and two semiflexible polymers. Curves have been shifted vertically for clarity. Cooling and heating rates are  $2.5 \times 10^{-4}$  in Lennard-Jones units.

flexibility the heating curves for the glass formed at low and high pressure. A measure of the effect of pressure densification is the dimensionless quantity  $\delta$  defined as<sup>34</sup>

$$\delta = \frac{v_{CG} - v_{PD}(P_0)}{v_{CG} - v_{PD}(P_1)} \quad (4)$$

where the specific volume  $v_{CG}$  of the CG is measured at low pressure  $P_0$  and that of the PD glass at  $P_0$  and at the (higher) densification pressure  $P_1$ . For real polymers,  $\delta$  spans values from 0.13 to 0.36.<sup>34,35</sup> The  $\delta$  in Figure 3 is in this range for chains with  $A \geq 5$ . More flexible chains show small or no effect of vitrification pressure; for a freely jointed chain (not shown), we find  $\delta = 0$ .

Also seen in Figure 3 is that the glass transition temperature, defined as the temperature at which the thermal expansion coefficient begins to increase during heating, is always lower for the PD glass. Thus, by either of the two criteria, the extent of densification or the stability of the glass, stiffer chains exhibit a larger effect of pressure densification, behavior comparable to real polymers.

The last property we investigate is isochronal superpositioning of the relaxation dispersion for the segmental dynamics and for the Johari–Goldstein secondary process. The Johari–Goldstein (JG) relaxation is a specific type of secondary relaxation, present in a wide variety of glass-forming liquids and polymers, which involves motion of all atoms in the molecule or polymer repeat unit<sup>36</sup> and some or all molecules depending on the material and temperature.<sup>37</sup> Several properties of the JG relaxation are related to the main  $\alpha$  relaxation,<sup>38</sup> one being that  $\tau_{JG}$  is constant for constant  $\tau_\alpha$  for many molecular liquids and their mixtures.<sup>39,40</sup> For polymers, however,  $\tau_{JG}$  decreases for constant  $\tau_\alpha$  with increasing  $T$  and  $P$ .<sup>18,19</sup> In Figure 4 are shown the first-order bond rotational

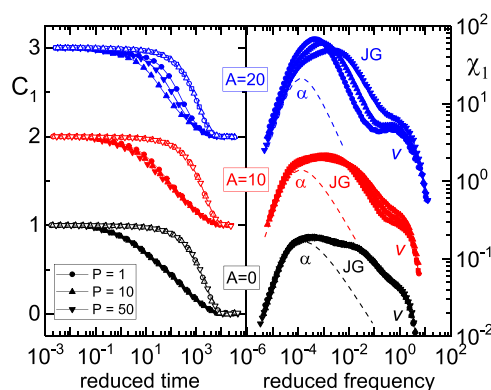


**Figure 4.** Dynamics in reduced units for the freely rotating and two semiflexible chains with length  $N = 16$  at the indicated pressures and at temperatures for which  $\bar{\tau}_\alpha \approx 10^3$  (along an  $\alpha$  relaxation isochrone). Left: rotational correlation function  $C_1$  (solid symbols) and end-to-end correlation function (empty symbols). Right: imaginary part of the susceptibility corresponding to  $C_1$ . Maxima for the  $\alpha$  and JG relaxations and vibrational modes are evident; the contribution of the  $\alpha$  relaxation to each  $P = 0$  spectrum is shown as the dotted line. For this chain length, the end-to-end relaxation does not result in a separate peak in  $\chi_1$ .

correlation function,  $C_1(t) = \langle \cos \theta(t) \rangle$  (where  $\theta(t)$  is the angular change of a bond vector) and its Fourier transform  $\chi_1$ , as well as the chain end-to-end correlation function. At each pressure, the temperature is determined that gives superpositioning of the segmental relaxation, to identify state points having constant  $\tau_\alpha$ . It is seen that a corresponding collapse of the full spectrum, which includes the JG relaxation, is obtained only for the freely rotating chain. There is no collapse for  $A > 0$  due to the JG relaxation having a different  $(T, P)$  dependence.

This breakdown of isochronal superpositioning for less flexible chains is brought out more clearly in the susceptibility spectra (right panel of Figure 4). The spectra were fit to a sum of three contributions: the local segmental dynamics, the JG process, and the vibrations. The segmental relaxation was described using the Kohlrausch function, with  $\tau_\alpha$  and the stretch exponent kept fixed. The latter follows from the invariance of the  $\alpha$  relaxation function at a fixed relaxation time.<sup>41,42</sup> As evident in the spectra in Figure 4, for  $A > 0$  there is a systematic increase in the frequency of the JG peak with increasing  $T$  and  $P$ . This breakdown of isochronal superpositioning corresponds to the behavior seen in experiments on polymers.<sup>17–19</sup>

## CONCLUSIONS

Molecular dynamics simulations of polymer chains reproduce the segmental dynamic properties of real polymers, provided there are constraints on the rotation about backbone bonds. The diminished effect of volume on the segmental dynamics at higher chain length, the capacity for pressure densification, and deviation from a constant JG relaxation time at constant  $\tau_\alpha$  all arise from torsional rigidity and become increasingly apparent for more rigid chains. Simulations of more flexible polymers, including freely jointed and freely rotating chains that lack a torsional potential, exhibit results for the  $\alpha$  relaxation that do not match experiments. The origin of the discordant behavior is the capacity of flexible chains to mitigate intermolecular constraints on their local motions, in this respect mimicking to some extent molecular liquids, with which they share the aforementioned properties. A similar effect can be seen in the

fragility (steepness in the temperature dependence of segmental relaxation), which is broadly in the same range as molecular liquids for flexible polymers with no side groups but typically higher for other polymers.<sup>43,44</sup> For polymers with side groups, the relative stiffness of side groups and the main chain appear to control fragility,<sup>44,45</sup> and it would be interesting to examine the effect of side groups on the three properties considered herein.

## AUTHOR INFORMATION

### Corresponding Author

\*E-mail: [daniel.fragiadakis@nrl.navy.mil](mailto:daniel.fragiadakis@nrl.navy.mil).

### ORCID

Daniel Fragiadakis: 0000-0002-0259-3677

C. Michael Roland: 0000-0001-7619-9202

### Notes

The authors declare no competing financial interest.

## ACKNOWLEDGMENTS

This work was supported by the Office of Naval Research.

## REFERENCES

- (1) Dyre, J. C. Hidden Scale Invariance in Condensed Matter. *J. Phys. Chem. B* **2014**, *118*, 10007–10024.
- (2) Roland, C. M. Relaxation Phenomena in Vitriifying Polymers and Molecular Liquids. *Macromolecules* **2010**, *43*, 7875–7890.
- (3) Tölle, A. Neutron Scattering Studies of the Model Glass Former ortho-terphenyl. *Rep. Prog. Phys.* **2001**, *64*, 1473–1532.
- (4) Hollander, A. G. S.; Prins, K. O. Atactic Polypropylene at High Pressure. I. Deuteron-NMR Determination of the Glass-transition Temperature. *J. Non-Cryst. Solids* **2001**, *286*, 1–11.
- (5) Casalini, R.; Roland, C. M. Thermodynamical Scaling of the Glass Transition Dynamics. *Phys. Rev. E* **2004**, *69*, No. 062501.
- (6) Dreyfus, C.; Le Grand, A.; Gapinski, J.; Steffen, W.; Patkowski, A. Scaling the  $\alpha$ -Relaxation Time of Supercooled Fragile Organic Liquids. *Eur. Phys. J. B* **2004**, *42*, 309–319.
- (7) Alba-Simionesco, C.; Cailliaux, A.; Alegria, A.; Tarjus, G. Scaling Out the Density Dependence of the  $\alpha$  Relaxation in Glass-Forming Polymers. *Europhys. Lett.* **2004**, *68*, 58–64.
- (8) Roland, C. M. *Viscoelastic Behavior of Rubbery Materials*; Oxford University Press, 2011; Chapter 3.
- (9) Jain, S.; Larson, R. G. Effects of Bending and Torsional Potentials on High-Frequency Viscoelasticity of Dilute Polymer Solutions. *Macromolecules* **2008**, *41*, 3692–3700.
- (10) Gee, R. H.; Boyd, R. H. The Role of the Torsional Potential in Relaxation Dynamics: a Molecular Dynamics study of Polyethylene. *Comput. Theor. Polym. Sci.* **1998**, *8*, 93–98.
- (11) Glotzer, S. C.; Paul, W. Molecular and Mesoscale Simulation Methods for Polymer Materials. *Annu. Rev. Mater. Res.* **2002**, *32*, 401–436.
- (12) Bedrov, D.; Smith, G. D. Secondary Johari–Goldstein Relaxation in Linear Polymer Melts Represented by a Simple Bead-Necklace model. *J. Non-Cryst. Solids* **2011**, *357*, 258–263.
- (13) Casalini, R.; Roland, C. M.; Capaccioli, S. Effect of Chain Length on Fragility and Thermodynamic Scaling of the Local Segmental Dynamics in Poly(methylmethacrylate). *J. Chem. Phys.* **2007**, *126*, No. 184903.
- (14) Casalini, R.; Roland, C. M. Density Scaling of the Structural and Johari–Goldstein Secondary Relaxations in Poly(methyl methacrylate). *Macromolecules* **2013**, *46*, 6364–6368.
- (15) Roland, C. M.; McGrath, K. J.; Casalini, R. Volume Effects on the Glass Transition Dynamics. *J. Non-Cryst. Solids* **2006**, *352*, 4910–4914.
- (16) Hutchinson, J. M. *The Physics of Glassy Polymers*; Haward, R. N., Ed.; Springer: NY, 1997.
- (17) Casalini, R.; Roland, C. M. Anomalous Properties of the Local Dynamics in Polymer Glasses. *J. Chem. Phys.* **2009**, *131*, No. 114501.
- (18) Casalini, R.; Roland, C. M. Density Scaling of the Structural and Johari–Goldstein Secondary Relaxations in Poly(methyl methacrylate). *Macromolecules* **2013**, *46*, 6364–6368.
- (19) Ransom, T. C.; Fragiadakis, D.; Roland, C. M. The  $\alpha$  and Johari–Goldstein Relaxations in 1,4-Polybutadiene: Breakdown of Isochronal Superpositioning. *Macromolecules* **2018**, *51*, 4694–4698.
- (20) Bailey, N.; Ingebrigtsen, T.; Hansen, J. S.; Veldhorst, A.; Böhring, L.; Lemarchand, C.; Olsen, A.; Bacher, A.; Costigliola, L.; Pedersen, U.; Larsen, H.; et al. RUMD: A General Purpose Molecular Dynamics Package Optimized to Utilize GPU Hardware Down to a Few Thousand Particles. *SciPost Phys.* **2017**, *3*, 038.
- (21) Nosé, S. A Unified Formulation of the Constant Temperature Molecular Dynamics Methods. *J. Chem. Phys.* **1984**, *81*, 511.
- (22) Berendsen, H. J.; Postma, J. V.; van Gunsteren, W. F.; DiNola, A. R. H. J.; Haak, J. R. Molecular Dynamics with Coupling to an External Bath. *J. Chem. Phys.* **1984**, *81*, 3684–3690.
- (23) Casalini, R.; Gamache, R. F.; Roland, C. M. Density-Scaling and the Prigogine–Defay Ratio in Liquids. *J. Chem. Phys.* **2011**, *135*, No. 224501.
- (24) Gnan, N.; Schröder, T. B.; Pedersen, U. R.; Bailey, N. P.; Dyre, J. C. Pressure-Energy Correlations in Liquids. IV. “Isomorphs” in Liquid Phase Diagrams. *J. Chem. Phys.* **2009**, *131*, No. 234504.
- (25) Fragiadakis, D.; Roland, C. M. On the Density Scaling of Liquid Dynamics. *J. Chem. Phys.* **2011**, *134*, No. 044504.
- (26) Veldhorst, A. Tests of the Isomorph Theory by Computer Simulations of Atomic and Molecular Model Liquids. Ph. D. Dissertation, Roskilde University: Roskilde Denmark, 2014.
- (27) Fragiadakis, D.; Roland, C. M. Intermolecular Distance and Density Scaling of Dynamics in Molecular Liquids. *J. Chem. Phys.* **2019**, *150*, No. 204501.
- (28) Grassia, L.; D’Amore, A. Isobaric and Isothermal Glass Transition of PMMA: Pressure-Volume-Temperature Experiments and Modelling Predictions. *J. Non-Cryst. Solids* **2011**, *357*, 414–418.
- (29) Schmidt, M.; Maurer, F. H. Isotropic Pressure-densified Atactic Poly(methyl methacrylate) Glasses: Free-volume Properties from Equation-of-state Data and Positron Annihilation Lifetime Spectroscopy. *Macromolecules* **2000**, *33*, 3879–3891.
- (30) Zoller, P.; Walsh, D. *Standard Pressure-Volume-Temperature Data for Polymers*; CRC Press, 1995.
- (31) Casalini, R. private communication.
- (32) Harmandaris, V. A.; Floudas, G.; Kremer, K. Temperature and Pressure Dependence of Polystyrene Dynamics Through Molecular Dynamics Simulations and Experiments. *Macromolecules* **2011**, *44*, 393–402.
- (33) Oels, H. J.; Rehage, G. Pressure-Volume-Temperature Measurements on Atactic Polystyrene. A thermodynamic view. *Macromolecules* **1977**, *10*, 1036–1043.
- (34) Fragiadakis, D.; Roland, C. M. A Test for the Existence of Isomorphs in Glass-forming Materials. *J. Chem. Phys.* **2017**, *147*, No. 084508.
- (35) Holt, A. P.; Fragiadakis, D.; Wollmerhauser, J. A.; Feigelson, B. N.; Tyagi, M.; Roland, C. M. Stability Limits of Pressure Densified Polycarbonate. *Macromolecules* **2019**, *52*, 4139.
- (36) Ngai, K. L.; Paluch, M. Classification of Secondary Relaxation in Glass-formers Based on Dynamic Properties. *J. Chem. Phys.* **2004**, *120*, 857.
- (37) Fragiadakis, D.; Roland, C. M. Participation in the Johari–Goldstein process: Molecular Liquids Versus Polymers. *Macromolecules* **2017**, *50*, 4039.
- (38) Ngai, K. L. Relaxation and Diffusion in Complex Systems. In *Partially Ordered Systems*; Springer, 2011.
- (39) Ngai, K. L.; Habasaki, J.; Prevosto, D.; Capaccioli, S.; Paluch, M. Thermodynamic Scaling of  $\alpha$ -relaxation Time and Viscosity Stems from the Johari–Goldstein  $\beta$ -relaxation or the Primitive Relaxation of the Coupling Model. *J. Chem. Phys.* **2012**, *137*, No. 034511.

(40) Thayyil, M. S.; Ngai, K. L.; Prevosto, D.; Capaccioli, S. Revealing the Rich Dynamics of Glass-Forming Systems by Modification of Composition and Change of Thermodynamic Conditions. *J. Non-Cryst. Solids* **2015**, *407*, 98–105.

(41) Roland, C. M.; Casalini, R.; Paluch, M. Isochronal Temperature-Pressure Superpositioning of the  $\alpha$ -relaxation in Type-A Glass Formers. *Chem. Phys. Lett.* **2003**, *367*, 259.

(42) Ngai, K. L.; Casalini, R.; Capaccioli, S.; Paluch, M.; Roland, C. M. Do Theories of the Glass Transition, in which the Structural Relaxation Time Does Not Define the Dispersion of the Structural Relaxation, Need Revision? *J. Phys. Chem. B* **2005**, *109*, 17356–17360.

(43) Dalle-Ferrier, C.; Kisluk, A.; Hong, L.; Carini, G., Jr.; Carini, G.; D'Angelo, G.; Alba-Simionesco, C.; Novikov, V. N.; Sokolov, A. P. Why Many Polymers Are so Fragile: A New Perspective. *J. Chem. Phys.* **2016**, *145*, No. 154901.

(44) Ngai, K. L.; Roland, C. M. Chemical Structure and Intermolecular Cooperativity: Dielectric Relaxation Results. *Macromolecules* **1993**, *26*, 6824–6830.

(45) Kunal, K.; Robertson, C. G.; Pawlus, S.; Hahn, S. F.; Sokolov, A. P. Role of Chemical Structure in Fragility of Polymers: A Qualitative Picture. *Macromolecules* **2008**, *41*, 7232–7238.